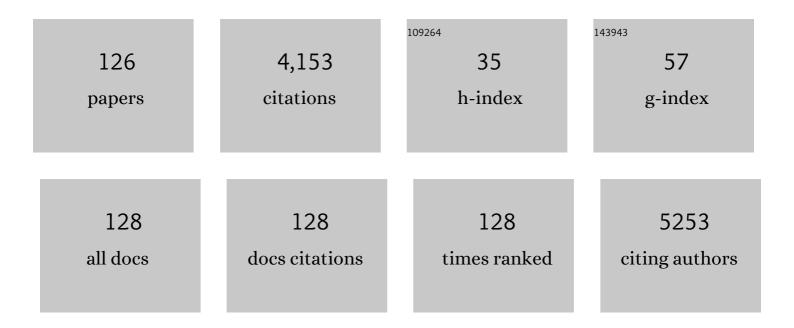
Sebastian Meier

List of Publications by Year in descending order

Source: https://exaly.com/author-pdf/8981677/publications.pdf Version: 2024-02-01



#	Article	IF	CITATIONS
1	Identification of slow correlated motions in proteins using residual dipolar and hydrogen-bond scalar couplings. Proceedings of the National Academy of Sciences of the United States of America, 2005, 102, 13885-13890.	3.3	220
2	Quantitative Description of Backbone Conformational Sampling of Unfolded Proteins at Amino Acid Resolution from NMR Residual Dipolar Couplings. Journal of the American Chemical Society, 2009, 131, 17908-17918.	6.6	187
3	Acetaldehyde as an Intermediate in the Electroreduction of Carbon Monoxide to Ethanol on Oxideâ€Derived Copper. Angewandte Chemie - International Edition, 2016, 55, 1450-1454.	7.2	166
4	Quantitative Determination of the Conformational Properties of Partially Folded and Intrinsically Disordered Proteins Using NMR Dipolar Couplings. Structure, 2009, 17, 1169-1185.	1.6	160
5	Foldon, The Natural Trimerization Domain of T4 Fibritin, Dissociates into a Monomeric A-state Form containing a Stable β-Hairpin: Atomic Details of Trimer Dissociation and Local β-Hairpin Stability from Residual Dipolar Couplings. Journal of Molecular Biology, 2004, 344, 1051-1069.	2.0	131
6	Evolution of complex structures: minicollagens shape the cnidarian nematocyst. Trends in Genetics, 2008, 24, 431-438.	2.9	117
7	A recycling pathway for cyanogenic glycosides evidenced by the comparative metabolic profiling in three cyanogenic plant species. Biochemical Journal, 2015, 469, 375-389.	1.7	109
8	Very Fast Folding and Association of a Trimerization Domain from Bacteriophage T4 Fibritin. Journal of Molecular Biology, 2004, 337, 905-915.	2.0	104
9	Conformational distributions of unfolded polypeptides from novel NMR techniques. Journal of Chemical Physics, 2008, 128, 052204.	1.2	88
10	Metabolic pathway visualization in living yeast by DNP-NMR. Molecular BioSystems, 2011, 7, 2834.	2.9	87
11	Mapping the Conformational Landscape of Urea-Denatured Ubiquitin Using Residual Dipolar Couplings. Journal of the American Chemical Society, 2007, 129, 9799-9807.	6.6	78
12	Tissue-specific Short Chain Fatty Acid Metabolism and Slow Metabolic Recovery after Ischemia from Hyperpolarized NMR in Vivo. Journal of Biological Chemistry, 2009, 284, 36077-36082.	1.6	76
13	Structural characterization of homogalacturonan by NMR spectroscopy—assignment of reference compounds. Carbohydrate Research, 2008, 343, 2830-2833.	1.1	75
14	Strategy for Nuclear-Magnetic-Resonance-Based Metabolomics of Human Feces. Analytical Chemistry, 2015, 87, 5930-5937.	3.2	69
15	Imaging of branched chain amino acid metabolism in tumors with hyperpolarized ¹³ C ketoisocaproate. International Journal of Cancer, 2010, 127, 729-736.	2.3	63
16	Real-time detection of central carbon metabolism in living <i>Escherichia coli</i> and its response to perturbations. FEBS Letters, 2011, 585, 3133-3138.	1.3	63
17	Charged acrylamide copolymer gels as media for weak alignment. Journal of Biomolecular NMR, 2002, 24, 351-356.	1.6	60
18	Development of Dissolution DNP-MR Substrates for Metabolic Research. Applied Magnetic Resonance, 2012, 43, 223-236.	0.6	60

#	Article	lF	CITATIONS
19	Study of molecular interactions with 13C DNP-NMR. Journal of Magnetic Resonance, 2010, 203, 52-56.	1.2	59
20	Continuous Molecular Evolution of Protein-Domain Structures by Single Amino Acid Changes. Current Biology, 2007, 17, 173-178.	1.8	56
21	Tin-containing silicates: identification of a glycolytic pathway via 3-deoxyglucosone. Green Chemistry, 2016, 18, 3360-3369.	4.6	56
22	Direct Observation of Dipolar Couplings and Hydrogen Bonds across a Î ² -Hairpin in 8 M Urea. Journal of the American Chemical Society, 2007, 129, 754-755.	6.6	54
23	Oxidative Depolymerization of Kraft Lignin for Microbial Conversion. ACS Sustainable Chemistry and Engineering, 2019, 7, 11640-11652.	3.2	51
24	Hyperpolarized Amino Acids for In Vivo Assays of Transaminase Activity. Chemistry - A European Journal, 2009, 15, 10010-10012.	1.7	50
25	Discovery of fungal oligosaccharide-oxidising flavo-enzymes with previously unknown substrates, redox-activity profiles and interplay with LPMOs. Nature Communications, 2021, 12, 2132.	5.8	50
26	Chemodiversity of Ladder-Frame Prymnesin Polyethers in <i>Prymnesium parvum</i> . Journal of Natural Products, 2016, 79, 2250-2256.	1.5	47
27	Hyperpolarized NMR Probes for Biological Assays. Sensors, 2014, 14, 1576-1597.	2.1	46
28	Detection of low-populated reaction intermediates with hyperpolarized NMR. Chemical Communications, 2009, , 5168.	2.2	44
29	Synergistic amylomaltase and branching enzyme catalysis to suppress cassava starch digestibility. Carbohydrate Polymers, 2015, 132, 409-418.	5.1	44
30	Specific and Nonspecific Interactions in Ultraweak Protein–Protein Associations Revealed by Solvent Paramagnetic Relaxation Enhancements. Journal of the American Chemical Society, 2014, 136, 10277-10286.	6.6	41
31	NMR Insights into the Inner Workings of Living Cells. Analytical Chemistry, 2015, 87, 119-132.	3.2	41
32	Acetaldehyde as an Intermediate in the Electroreduction of Carbon Monoxide to Ethanol on Oxideâ€Derived Copper. Angewandte Chemie, 2016, 128, 1472-1476.	1.6	39
33	Minicollagen-15, a Novel Minicollagen Isolated from Hydra, Forms Tubule Structures in Nematocysts. Journal of Molecular Biology, 2008, 376, 1008-1020.	2.0	38
34	Quantitative dynamic nuclear polarizationâ€NMR on blood plasma for assays of drug metabolism. NMR in Biomedicine, 2011, 24, 96-103.	1.6	37
35	Unmixing the NMR spectra of similar species – vive la différence. Chemical Communications, 2013, 49, 10510.	2.2	37
36	High-Accuracy Residual1HNâ^'13C and1HNâ^'1HNDipolar Couplings in Perdeuterated Proteins. Journal of the American Chemical Society, 2003, 125, 44-45.	6.6	36

#	Article	IF	CITATIONS
37	Structural Analysis of B-Box 2 from MuRF1: Identification of a Novel Self-Association Pattern in a RING-like Fold. Biochemistry, 2008, 47, 10722-10730.	1.2	36
38	A biological cosmos of parallel universes: Does protein structural plasticity facilitate evolution?. BioEssays, 2007, 29, 1095-1104.	1.2	35
39	Combined Function of BrÃ,nsted and Lewis Acidity in the Zeoliteâ€Catalyzed Isomerization of Glucose to Fructose in Alcohols. ChemCatChem, 2016, 8, 3107-3111.	1.8	35
40	Direct Observation of Metabolic Differences in Living <i>Escherichia Coli</i> Strains Kâ€12 and BL21. ChemBioChem, 2012, 13, 308-310.	1.3	34
41	Structure of branching enzyme- and amylomaltase modified starch produced from well-defined amylose to amylopectin substrates. Carbohydrate Polymers, 2016, 152, 51-61.	5.1	34
42	Karmitoxin: An Amine-Containing Polyhydroxy-Polyene Toxin from the Marine Dinoflagellate Karlodinium armiger. Journal of Natural Products, 2017, 80, 1287-1293.	1.5	34
43	Fast and Accurate Quantitation of Glucans in Complex Mixtures by Optimized Heteronuclear NMR Spectroscopy. Analytical Chemistry, 2013, 85, 8802-8808.	3.2	33
44	Functional and structural characterization of plastidic starch phosphorylase during barley endosperm development. PLoS ONE, 2017, 12, e0175488.	1.1	33
45	Kinetic analysis of hexose conversion to methyl lactate by Sn-Beta: effects of substrate masking and of water. Catalysis Science and Technology, 2018, 8, 2137-2145.	2.1	33
46	Shapeâ€selective Valorization of Biomassâ€derived Glycolaldehyde using Tinâ€containing Zeolites. ChemSusChem, 2016, 9, 3054-3061.	3.6	31
47	Control of selectivity in hydrosilane-promoted heterogeneous palladium-catalysed reduction of furfural and aromatic carboxides. Communications Chemistry, 2018, 1, .	2.0	31
48	Solventâ€Activated Hafnium ontaining Zeolites Enable Selective and Continuous Glucose–Fructose Isomerisation. Angewandte Chemie - International Edition, 2020, 59, 20017-20023.	7.2	31
49	Ultrahigh-Resolution Backbone Structure of Perdeuterated Protein GB1 Using Residual Dipolar Couplings from Two Alignment Media. Angewandte Chemie - International Edition, 2006, 45, 8166-8169.	7.2	30
50	Detecting Beer Intake by Unique Metabolite Patterns. Journal of Proteome Research, 2016, 15, 4544-4556.	1.8	30
51	Synthesis of a novel polyester building block from pentoses by tin-containing silicates. RSC Advances, 2017, 7, 985-996.	1.7	29
52	Quantitative NMR Approach to Optimize the Formation of Chemical Building Blocks from Abundant Carbohydrates. ChemSusChem, 2017, 10, 2990-2996.	3.6	29
53	The Structure of the Cys-rich Terminal Domain of Hydra Minicollagen, Which Is Involved in Disulfide Networks of the Nematocyst Wall. Journal of Biological Chemistry, 2004, 279, 30395-30401.	1.6	28
54	Profiling of carbohydrate mixtures at unprecedented resolution using high-precision ¹ H- ¹³ C chemical shift measurements and a reference library. Analyst, The, 2014, 139, 401-406.	1.7	28

#	Article	IF	CITATIONS
55	Noble metal-free upgrading of multi-unsaturated biomass derivatives at room temperature: silyl species enable reactivity. Green Chemistry, 2018, 20, 5327-5335.	4.6	28
56	Sequence–Structure and Structure–Function Analysis in Cysteine-rich Domains Forming the Ultrastable Nematocyst Wall. Journal of Molecular Biology, 2007, 368, 718-728.	2.0	27
57	NMR characterization of chemically synthesized branched α-dextrin model compounds. Carbohydrate Research, 2015, 403, 149-156.	1.1	25
58	Oxidative Depolymerisation of Lignosulphonate Lignin into Low-Molecular-Weight Products with Cu–Mn/δ-Al2O3. Topics in Catalysis, 2019, 62, 639-648.	1.3	25
59	Developing Inhibitors of the p47phox–p22phox Protein–Protein Interaction by Fragment-Based Drug Discovery. Journal of Medicinal Chemistry, 2020, 63, 1156-1177.	2.9	25
60	Oxidative depolymerization of Kraft lignin to high-value aromatics using a homogeneous vanadium–copper catalyst. Catalysis Science and Technology, 2021, 11, 1843-1853.	2.1	24
61	High-Resolution Structure of the Histidine-Containing Phosphocarrier Protein (HPr) from Staphylococcus aureus and Characterization of Its Interaction with the Bifunctional HPr Kinase/Phosphorylase. Journal of Bacteriology, 2004, 186, 5906-5918.	1.0	22
62	1H NMR spectroscopy for profiling complex carbohydrate mixtures in non-fractionated beer. Food Chemistry, 2014, 150, 65-72.	4.2	21
63	Spectroscopic studies of the interactions between β-lactoglobulin and bovine submaxillary mucin. Food Hydrocolloids, 2015, 50, 203-210.	5.6	21
64	Mechanism and stereoselectivity of zeolite-catalysed sugar isomerisation in alcohols. Chemical Communications, 2016, 52, 12773-12776.	2.2	20
65	Realâ€Time DNP NMR Observations of Acetic Acid Uptake, Intracellular Acidification, and of Consequences for Glycolysis and Alcoholic Fermentation in Yeast. Chemistry - A European Journal, 2013, 19, 13288-13293.	1.7	19
66	Depolymerization of fucoidan with endo-fucoidanase changes bioactivity in processes relevant for bone regeneration. Carbohydrate Polymers, 2022, 286, 119286.	5.1	18
67	Facile and benign conversion of sucrose to fructose using zeolites with balanced BrÃ,nsted and Lewis acidity. Catalysis Science and Technology, 2017, 7, 2782-2788.	2.1	17
68	Effects of Alkaliâ€Metal Ions and Counter Ions in Snâ€Beta atalyzed Carbohydrate Conversion. ChemSusChem, 2018, 11, 1198-1203.	3.6	17
69	Metabolic Fate of ¹³ C-Labeled Polydextrose and Impact on the Gut Microbiome: A Triple-Phase Study in a Colon Simulator. Journal of Proteome Research, 2018, 17, 1041-1053.	1.8	17
70	NMR Spectroscopic Isotope Tracking Reveals Cascade Steps in Carbohydrate Conversion by Tinâ€Beta. ChemCatChem, 2018, 10, 1414-1419.	1.8	17
71	Selective Enzymatic Release and Gel Formation by Cross-Linking of Feruloylated Glucurono-Arabinoxylan from Corn Bran. ACS Sustainable Chemistry and Engineering, 2020, 8, 8164-8174.	3.2	17
72	Timeâ€Resolved in‣itu Observation of Starch Polysaccharide Degradation Pathways. ChemBioChem, 2013, 14, 2506-2511.	1.3	16

#	Article	IF	CITATIONS
73	Probing Interactions between β-Glucan and Bile Salts at Atomic Detail by ¹ H– ¹³ C NMR Assays. Journal of Agricultural and Food Chemistry, 2014, 62, 11472-11478.	2.4	16
74	Determination of a high-precision NMR structure of the minicollagen cysteine rich domain fromHydraand characterization of its disulfide bond formation. FEBS Letters, 2004, 569, 112-116.	1.3	15
75	Development of brewing science in (and since) the late 19th century: Molecular profiles of 110–130year old beers. Food Chemistry, 2015, 183, 227-234.	4.2	15
76	Mechanism and malleability of glucose dehydration to HMF: entry points and water-induced diversions. Catalysis Science and Technology, 2020, 10, 1724-1730.	2.1	15
77	The structure of the AliC GH13 α-amylase from <i>Alicyclobacillus</i> sp. reveals the accommodation of starch branching points in the α-amylase family. Acta Crystallographica Section D: Structural Biology, 2019, 75, 1-7.	1.1	15
78	Probing Helical Hydrophobic Binding Sites in Branched Starch Polysaccharides Using NMR Spectroscopy. Chemistry - A European Journal, 2013, 19, 16314-16320.	1.7	14
79	Simultaneous Determination of Binding Constants for Multiple Carbohydrate Hosts in Complex Mixtures. Journal of the American Chemical Society, 2014, 136, 11284-11287.	6.6	14
80	Ammonia borane enabled upgrading of biomass derivatives at room temperature. Green Chemistry, 2020, 22, 5972-5977.	4.6	14
81	Backbone resonance assignment of the 298 amino acid catalytic domain of protein tyrosine phosphatase 1B (PTP1B). Journal of Biomolecular NMR, 2002, 24, 165-166.	1.6	12
82	Monitoring pathways of β-glucan degradation by enzyme mixtures in situ. Carbohydrate Research, 2013, 368, 47-51.	1.1	12
83	Modification of commercial Y zeolites by alkaline-treatment for improved performance in the isomerization of glucose to fructose. Molecular Catalysis, 2021, 510, 111686.	1.0	12
84	Sulfite Action in Glycolytic Inhibition: In Vivo Realâ€īime Observation by Hyperpolarized ¹³ C NMR Spectroscopy. ChemBioChem, 2012, 13, 2265-2269.	1.3	11
85	Discovery and Exploration of the Efficient Acyclic Dehydration of Hexoses in Dimethyl Sulfoxide/Water. ChemSusChem, 2019, 12, 5086-5091.	3.6	11
86	The Endo-α(1,4) Specific Fucoidanase Fhf2 From Formosa haliotis Releases Highly Sulfated Fucoidan Oligosaccharides. Frontiers in Plant Science, 2022, 13, 823668.	1.7	11
87	Determination of native capsular polysaccharide structures of Streptococcus pneumoniae serotypes 39, 42, and 47F and comparison to genetically or serologically related strains. Carbohydrate Research, 2014, 395, 38-46.	1.1	10
88	Stoichiometric active site modification observed by alkali ion titrations of Sn-Beta. Catalysis Science and Technology, 2019, 9, 4339-4346.	2.1	10
89	Probing the Lewis Acid Catalyzed Acyclic Pathway of Carbohydrate Conversion in Methanol by <i>In Situ</i> NMR. ChemCatChem, 2019, 11, 5077-5084.	1.8	10
90	Catalytic cycle of carbohydrate dehydration by Lewis acids: structures and rates from synergism of conventional and DNP NMR. Chemical Communications, 2020, 56, 6245-6248.	2.2	10

#	Article	IF	CITATIONS
91	Antibody glycans wiggle and jiggle. Nature Chemical Biology, 2011, 7, 131-132.	3.9	9
92	Probing the structural details of xylan degradation by real-time NMR spectroscopy. Carbohydrate Polymers, 2014, 112, 587-594.	5.1	9
93	Detecting Elusive Intermediates in Carbohydrate Conversion: A Dynamic Ensemble of Acyclic Glucose–Catalyst Complexes. ACS Sustainable Chemistry and Engineering, 2017, 5, 5571-5577.	3.2	9
94	Exploring the Synthesis of Mesoporous Stannosilicates as Catalysts for the Conversion of Mono- and Oligosaccharides into Methyl Lactate. Topics in Catalysis, 2019, 62, 628-638.	1.3	9
95	Enhanced 13C NMR detects extended reaction networks in living cells. Chemical Communications, 2021, 57, 10572-10575.	2.2	9
96	Mechanistic Studies of Continuous Glucose Upgrading over Lewis Acidic Silicates by <i>Operando</i> UV–Vis and HSQC NMR. ACS Catalysis, 2021, 11, 1296-1308.	5.5	9
97	Insights into Ammonia Borane-Enabled Green Synthesis of <i>N</i> -Substituted Lactams from Biomass-Derived Keto Acids and Amines. ACS Sustainable Chemistry and Engineering, 2021, 9, 4377-4382.	3.2	9
98	The Endo-α(1,3)-Fucoidanase Mef2 Releases Uniquely Branched Oligosaccharides from Saccharina latissima Fucoidans. Marine Drugs, 2022, 20, 305.	2.2	9
99	pH- and concentration-dependent supramolecular assembly of a fungal defensin plectasin variant into helical non-amyloid fibrils. Nature Communications, 2022, 13, .	5.8	9
100	Barley genotypic β-glucan variation combined with enzymatic modifications direct its potential as a natural ingredient in a high fiber extract. Journal of Cereal Science, 2017, 75, 45-53.	1.8	8
101	Combined In-Cell NMR and Simulation Approach to Probe Redox-Dependent Pathway Control. Analytical Chemistry, 2019, 91, 5395-5402.	3.2	8
102	Response Factors Enable Rapid Quantitative 2D NMR Analysis in Catalytic Biomass Conversion to Renewable Chemicals. Topics in Catalysis, 2019, 62, 590-598.	1.3	8
103	Adiabatic Lowâ€Pass J Filters for Artifact Suppression in Heteronuclear NMR. ChemPhysChem, 2009, 10, 893-895.	1.0	7
104	Recent progress in heteronuclear long-range NMR of complex carbohydrates: 3D H2BC and clean HMBC. Carbohydrate Research, 2009, 344, 2274-2278.	1.1	7
105	NMR assignment of structural motifs in intact β-limit dextrin and its α-amylase degradation products in situ. Carbohydrate Research, 2012, 359, 76-80.	1.1	7
106	In-situ annotation of carbohydrate diversity, abundance, and degradability in highly complex mixtures using NMR spectroscopy. Analytical and Bioanalytical Chemistry, 2014, 406, 7763-7772.	1.9	7
107	Spectroscopic approaches to resolving ambiguities of hyper-polarized NMR signals from different reaction cascades. Analyst, The, 2016, 141, 823-826.	1.7	7
108	Uncharted Pathways for CrCl3 Catalyzed Glucose Conversion in Aqueous Solution. Topics in Catalysis, 2019, 62, 669-677.	1.3	7

#	Article	IF	CITATIONS
109	Ru-Catalyzed Oxidative Cleavage of Guaiacyl GlycerolGuaiacyl Ether-a Representative -O-4 Lignin Model Compound. Catalysts, 2019, 9, 832.	1.6	7
110	Kinetic variations in acid-catalyzed monosaccharide conversion. Catalysis Communications, 2020, 135, 105894.	1.6	7
111	Versatile Procedures for Reliable NMR Quantification of CO ₂ Electroreduction Products. Journal of Physical Chemistry C, 2022, 126, 11026-11032.	1.5	7
112	3D H2BC: A novel experiment for small-molecule and biomolecular NMR at natural isotopic abundance. Journal of Magnetic Resonance, 2009, 200, 340-343.	1.2	6
113	Hyperpolarised organic phosphates as NMR reporters of compartmental pH. Chemical Communications, 2016, 52, 2288-2291.	2.2	6
114	Solventâ€Activated Hafniumâ€Containing Zeolites Enable Selective and Continuous Glucose–Fructose Isomerisation. Angewandte Chemie, 2020, 132, 20192-20198.	1.6	6
115	Structural determination of Streptococcus pneumoniae repeat units in serotype 41A and 41F capsular polysaccharides to probe gene functions in the corresponding capsular biosynthetic loci. Carbohydrate Research, 2014, 400, 26-32.	1.1	5
116	Supramolecular chemical shift reagents inducing conformational transitions: NMR analysis of carbohydrate homooligomer mixtures. Chemical Communications, 2015, 51, 3073-3076.	2.2	5
117	¹ H– ¹³ C NMR-Based Profiling of Biotechnological Starch Utilization. Analytical Chemistry, 2016, 88, 9685-9690.	3.2	5
118	Shape-selective Valorization of Biomass-derived Glycolaldehyde using Tin-containing Zeolites. ChemSusChem, 2016, 9, 3022-3022.	3.6	5
119	Pancreatic Î ² -cells respond to fuel pressure with an early metabolic switch. Scientific Reports, 2020, 10, 15413.	1.6	5
120	Heterogeneous Baseâ€Catalyzed Conversion of Glycolaldehyde to Aldotetroses: Mechanistic and Kinetic Insight. ChemCatChem, 2021, 13, 5141-5147.	1.8	5
121	Visualization of Pathway Usage in an Extended Carbohydrate Conversion Network Reveals the Impact of Solvent-Enabled Proton Transfer. ACS Sustainable Chemistry and Engineering, 2020, 8, 12270-12276.	3.2	4
122	Reactivity of Polysilazanes Allows Catalystâ€Free Curing of Silicones. Macromolecular Materials and Engineering, 2022, 307, .	1.7	4
123	Nuclear magnetic resonance as a quantitative tool to study interactions in biomacromolecules. Pure and Applied Chemistry, 2005, 77, 1409-1424.	0.9	3
124	Phosphocholine-Decorated PPI-Dendrimers Mimic Cell Membrane Phosphocholine Clusters and Tune the Innate Immune Activity of C-Reactive Protein. Biomacromolecules, 2021, 22, 1664-1674.	2.6	2
125	Sensitive NMR method for detecting carbohydrate influx into competing chemocatalytic pathways. Analyst, The, 2020, 145, 4427-4431.	1.7	0
126	Chemodiversity of the ladder-frame prymnesin polyethers of the fish-killing microalgal Prymnesium parvum. Planta Medica, 2016, 81, S1-S381.	0.7	0